Noncollinear cluster magnetism in the framework of the Hubbard model

Miguel A. Ojeda and J. Dorantes-Dávila
Instituto de Física, Universidad Autónoma de San Luis Potosí, Alvaro Obregón 64, 78000 San Luis Potosí, Mexico

G. M. Pastor
Laboratoire de Physique Quantique, Unité Mixte de Recherche 5626 du CNRS, Université Paul Sabatier, 118 route de Narbonne, F-31062 Toulouse, France

(Received 30 December 1998; revised manuscript received 11 May 1999)

Noncollinear magnetic states in clusters having $N \leqslant 43$ atoms are studied by using the single-band Hubbard Hamiltonian within the fully unrestricted Hartree-Fock (UHF) approximation. The spin and charge degrees of freedom $\langle \vec{S}_l \rangle$ and $\langle n_l \rangle$ at every cluster atom are treated as independent variables. A variety of qualitatively different self-consistent solutions is obtained as a function of cluster size, structure, number of valence electrons ν, and Coulomb interaction strength U/t. This includes inhomogeneous density distributions, paramagnetic solutions, magnetic solutions with collinear moments, and noncollinear spin arrangements that show complex antiferromagneticlike or ferromagneticlike orders. The environment dependence of the magnetic properties is analyzed giving emphasis to the effects of antiferromagnetic frustrations in compact structures close to half-band filling. Electron correlation effects are quantified by comparing UHF and exact results for the local magnetic moments, total spin, spin-correlation functions, and structural stability of 13-atom clusters. Goals and limitations of the present noncollinear approach are discussed. [S0163-1829(99)06131-7]

I. INTRODUCTION

Clusters may show specific phenomena that do not have an equivalent in the thermodynamic limit and that are therefore of interest in both basic and applied science. Moreover, the evolution of their physical properties with increasing cluster size provides new perspectives for understanding the microscopic origin of condensed-matter properties.[1] In this context, the study of magnetism in metals is a particularly interesting and challenging problem, since the properties of magnetic metals often change dramatically as the electrons of an isolated atom become part of a cluster of several atoms and delocalize. It is therefore of fundamental importance to understand how itinerant magnetism, as found for example in $3d$ transition-metal (TM) solids, develops starting from localized atomic magnetic moments. The strong dependence of the magnetic behavior as a function of size, structure, and composition opens up, in addition, the possibility of using clusters to tailor new magnetic materials for specific technological purposes. Consequently, the relation between local atomic environment, cluster structure, and magnetism also has implications of practical interest.

Most theoretical studies of itinerant cluster magnetism have been performed using Hartree-Fock (HF) and local spin-density (LSD) methods.[2,3] Exact many-body calculations are presently limited to simple models, such as the Hubbard model, and to systems containing a small number of sites.[4–6] Within mean-field approximations (HF or LSD) the self-consistent spin polarizations are usually restricted to be collinear, i.e., the direction of all local magnetic moments is assumed to be the same. However, the well-known sensitivity of itinerant magnetism to the local environment of the atoms[2,3] suggests that other instabilities towards spiral-like spin-density waves[7] (SDW's) or even more complex magnetic structures should also be possible in general. For example, the tendency to antiferromagnetic (AF) order close to half-band filling and the presence of triangular loops in compact structures generates magnetic frustrations that may easily yield complex arrangements of the local magnetic moments. Moreover, the reduction of local coordination numbers at the surface of clusters removes constraints between the local moments and could favor the development of low-symmetry spin polarizations. In solids, noncollinear magnetic structures have been identified experimentally and theoretically already for a long time.[7–11] In contrast, very little is known at present in the case of finite systems.[12–14] Fully unrestricted *ab initio* calculations of noncollinear spin arrangements have been performed only recently for very small Fe_N clusters.[14] The investigation of magnetic phenomena of this kind requires a symmetry unrestricted approach in which no *a priori* assumptions are made concerning the relative orientation of the local magnetic moments, thereby enlarging the number of degrees of freedom of the problem.

The possibility of developing noncollinear magnetic structures in small clusters should also have direct implications for the comparison between theory and experiment. Stern-Gerlach deflection measurements indicate that the average magnetic moments $\overline{\mu}_N$ in Cr_N and V_N clusters are very small, eventually vanishing [$\overline{\mu}_N \leqslant 0.7\mu_B$ for Cr_N and V_N (Ref. 15)]. State of the art collinear-spin calculations[3] yield large local magnetic moments μ_l showing AF order. In spite of the partial cancellations between different μ_l implied by antiferromagnetism, the $\overline{\mu}_N$ obtained by these methods are generally larger than the experimental values.[15] It would be therefore of interest to investigate to what extent the formation of noncollinear magnetic arrangements yields a more complete cancellation among the local spin polarizations, thus reducing $\overline{\mu}_N$.

The main purpose of this paper is to investigate the characteristics of noncollinear magnetic states in finite compact

clusters. We consider the single-band Hubbard model and determine the ground-state magnetic properties in the fully unrestricted Hartree-Fock approximation. The theoretical approach, outlined in Sec. II, is applied to clusters having $N \leqslant 43$ atoms. The results presented in Sec. III analyze noncollinear magnetic behaviors for a few representative compact structures. Several examples are given that illustrate the large variety of three-dimensional magnetic arrangements obtained in the self-consistent calculations as a function of the Coulomb repulsion strength U/t, band filling ν/N, and structure. In Sec. IV we compare the UHF results with exact diagonalization calculations for $N=13$ atoms (Lanczos method).[6] The role of quantum fluctuations beyond the mean field and the consequences of the often artificial breaking of spin symmetry implied by the formation of the noncollinear local moments are discussed. Taking into account that approximations such as UHF are unavoidable for larger clusters and for more realistic model Hamiltonians, it is of considerable interest to test the validity of these methods in order to improve the interpretation of the approximate results and to obtain a more accurate description of magnetic phenomena in clusters.

II. THEORETICAL METHOD

The single-band Hubbard Hamiltonian[16] is given by

$$H=-t\sum_{\langle l,m\rangle,\sigma}\hat{c}^{\dagger}_{l\sigma}\hat{c}_{m\sigma}+U\sum_{l}\hat{n}_{l\uparrow}\hat{n}_{l\downarrow}, \tag{2.1}$$

where $\hat{c}^{\dagger}_{l\sigma}$ ($\hat{c}_{l\sigma}$) is the creation (annihilation) operator of an electron at site l with spin σ, and $\hat{n}_{l\sigma}=\hat{c}^{\dagger}_{l\sigma}\hat{c}_{l\sigma}$ is the corresponding number operator ($\hat{n}_l=\Sigma_\sigma\hat{n}_{l\sigma}$). The first sum runs over all pairs of nearest neighbors (NN) and the second over all sites. The model is characterized by the dimensionless parameter U/t, which measures the relative importance between kinetic and Coulomb energies, by the cluster structure, which defines the kinetic energy operator, and by the number of valence electrons ν. The variations of U/t can be associated with a uniform relaxation of the interatomic distances (e.g., $t\propto R_{ij}^{-5}$ for TM's) or with changes in the spatial extension of the atomiclike wave function, as in different elements within the same group. Different ν's correspond to different band fillings ν/N that may be associated qualitatively with the variations of ν/N across a TM d series. In spite of its simplicity, this Hamiltonian has played, together with related models, a major role in guiding our understanding of the many-body properties of metals and of low-dimensional magnetism. It is the purpose of this work to use it to investigate the properties of noncollinear itinerant magnetism in small compact clusters.

In the unrestricted Hartree-Fock approximation H is replaced by the single-particle Hamiltonian[7,11,12]

$$H_{\mathrm{UHF}}=-t\sum_{\langle lm\rangle\sigma}c^{\dagger}_{l\sigma}c_{m\sigma}+U\sum_{l\sigma}\left(\rho_{l\sigma,l\sigma}\;c^{\dagger}_{l\bar{\sigma}}c_{l\bar{\sigma}}-\rho_{l\sigma,l\bar{\sigma}}\;c^{\dagger}_{l\bar{\sigma}}c_{l\sigma}\right), \tag{2.2}$$

from which a single-determinant approximation $|\mathrm{UHF}\rangle$ to the ground state is obtained. In Eq. (2.2), $\rho_{l\sigma,l\sigma'}$ are the matrix elements $\rho_{l\sigma,l\sigma'}=\langle c^{\dagger}_{l\sigma}c_{l\sigma'}\rangle$ of the density matrix, where $\langle\cdots\rangle=\langle\mathrm{UHF}|\cdots|\mathrm{UHF}\rangle$ implies self-consistency. The distribution of the electron density is given by

$$\langle n_l\rangle=\rho_{l\uparrow,l\uparrow}+\rho_{l\downarrow,l\downarrow}, \tag{2.3}$$

and the spin polarization $\langle\vec{S}_l\rangle=(S^x_l,S^y_l,S^z_l)$ by

$$\begin{aligned}\langle S^x_l\rangle&=(\rho_{l\uparrow,l\downarrow}+\rho_{l\downarrow,l\uparrow})/2,\\ \langle S^y_l\rangle&=-i\;(\rho_{l\uparrow,l\downarrow}-\rho_{l\downarrow,l\uparrow})/2,\\ \langle S^z_l\rangle&=(\rho_{l\uparrow,l\uparrow}-\rho_{l\downarrow,l\downarrow})/2.\end{aligned} \tag{2.4}$$

Notice that the local magnetic moments $\langle\vec{S}_l\rangle$ are collinear if $\rho_{l\sigma,l\bar{\sigma}}=0\;\;\forall\;\;l$.

The UHF energy can be rewritten as

$$E_{\mathrm{UHF}}=-t\sum_{\langle l,m\rangle,\sigma}\rho_{l\sigma,m\sigma}+\frac{U}{4}\sum_{l}\langle n_l\rangle^2-U\sum_{l}|\langle\vec{S}_l\rangle|^2. \tag{2.5}$$

One observes that the Hartree-Fock Coulomb energy E_C^{HF}—the sum of the second and third terms in Eq. (2.5)—favors a uniform density distribution and the formation of local moments $\langle\vec{S}_l\rangle$. Due to the local character of Hubbard's Coulomb interaction, the relative orientation of different $\langle\vec{S}_l\rangle$ does not affect E_C^{HF}. It is therefore the optimization of the kinetic energy that eventually leads to the formation of complex magnetic structures with $|\langle\vec{S}_l\rangle\cdot\langle\vec{S}_m\rangle|\neq 1$ or to nonuniform density distributions $\langle n_l\rangle$.

The UHF equations often allow multiple self-consistent solutions which correspond to different magnetic behaviors. It is therefore important to ensure that the final results correspond to the true UHF ground state. The situation is particularly delicate in our calculations since we allow a complete, independent rearrangement of the charge and spin degrees of freedom at every atomic site and since in low-symmetry clusters the spin structure is very difficult to infer *a priori*. In practice, several random spin arrangements (typically, 5–10) are used as starting points of the self-consistent procedure for each considered value of U/t. Moreover, the different solutions are followed as a function of U with small increments ΔU (depending on the situation $|\Delta U|/t=0.01$–0.1). Finally, the corresponding UHF energies are compared, in case of multiple solutions for a given U/t, and the numerical stability of the results is verified.

As a consequence of the tendency to avoid double orbital occupancies, the UHF solutions often correspond to states of broken symmetry: spin-density waves (SDW's), charge-density waves (CDW's), or both. The spin-rotational invariance of Eq. (2.2) implies that the energy is unchanged after a rotation of the whole spin arrangement $\{\langle\vec{S}_l\rangle,\; l=1,\ldots,N\}$. Therefore, if $\langle\vec{S}_l\rangle\neq 0$ one has a set of linearly independent congruent solutions $|\mathrm{UHF}k\rangle$ ($k\geqslant 2$) which have the same average energy E_{UHF} and which differ from each other only by the orientation of the spin polarizations relative to the cluster structure. The illustrations of spin arrangements shown in Sec. III correspond to one of these SDW's, which is chosen only for the sake of clarity. The set of UHF solu-

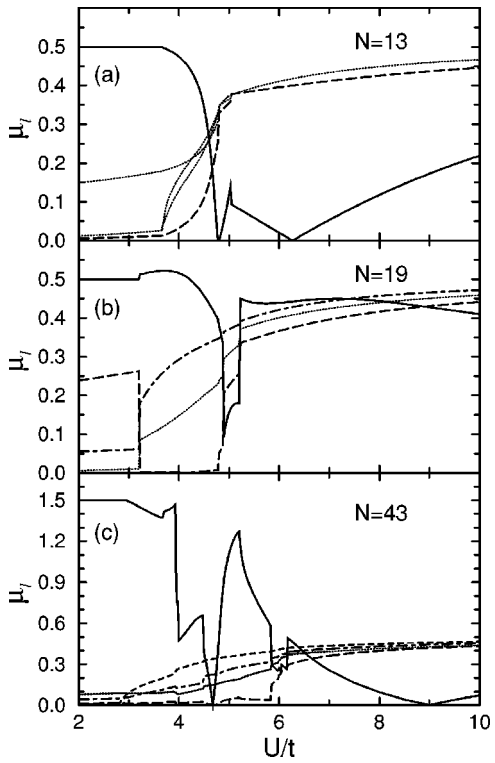

FIG. 1. Magnetic moments as a function of the Coulomb repulsion strength U/t for fcc-like clusters having (a) $N=13$, (b) $N=19$, and (c) $N=43$ atoms at half-band filling (UHF approximation). Local moments $\mu_l=|\langle\vec{S}_l\rangle|$ are shown for the central atom $l=1$ (dashed), its first NN's ($l=2$–13, dotted), second NN's ($l=14$–19, dashed-dotted), and third NN's ($l=20$–43, short dashed). In (b) and (c) μ_l refers to the shell average. The total moment $\mu_T=|\Sigma_l\langle\vec{S}_l\rangle|$ is given by the solid curves.

tions may be used to restore the symmetry appropriate to the exact ground state $|\Psi_0\rangle$ thereby improving the approximate wave function.[17,18]

In order to quantify the role of electron correlations and to assess goal and limitations of the UHF approximation in applications to finite clusters, we shall also compare some of our results with those obtained by applying exact diagonalization methods.[4–6]

III. NONCOLLINEAR MAGNETIC ORDER IN COMPACT CLUSTERS

A. Antiferromagnetic clusters

In Fig. 1 UHF results are given for the local magnetic moments $\mu_l=|\langle\vec{S}_l\rangle|$ and the total magnetic moment $\mu_T=|\Sigma_l\langle\vec{S}_l\rangle|$ of fcc-like clusters having $N=13$, 19, and 43 atoms at half-band filling ($\nu=N$). These clusters are formed by adding to a central atom ($l=1$) the successive shells of its first NN's ($N=13$), second NN's ($N=19$), and third NN's ($N=43$). Several common properties are observed as a function of U/t. Starting from the uncorrelated limit ($U=0$), the total moment μ_T remains approximately constant for $U/t\leqslant 3$–4. In the weakly interacting regime, the local moments μ_l do not depend strongly on U/t and are generally small. Notice that for $N=43$, μ_T is not minimal at small U ($\mu_T=3/2$) due to degeneracies in the single-particle spectrum. For larger U/t, μ_T decreases rapidly, eventually with some discontinuities and a few oscillations reaching values close to $\mu_T=0$ for $U/t\simeq 5$–6 ($U/t\simeq 9$ for $N=43$). At this intermediate range of U/t, the μ_l increase more rapidly, approaching saturation at the U/t for which μ_T is minimum ($\mu_l\simeq 0.40$–0.45). The opposite trends shown by μ_l and μ_T are a clear indication of the expected onset of strong AF-like order at half-band filling. We shall see in the following that this corresponds in fact to noncollinear spin arrangements. If U/t is increased beyond $U/t=5$–6 (beyond $U/t=9$ for $N=43$) the local moments do not vary significantly. The total moment μ_T either does not change very much ($N=19$) or increases monotonically with U/t ($N=13$ and 43) remaining always smaller than 1/2.

The almost complete cancellation of rather large local moments is qualitatively in agreement with experiments on TM's having a half-filled or nearly half-filled d band, such as Cr and V. Stern-Gerlach measurements[15] indicate that Cr_N and V_N clusters show very small, eventually vanishing, average magnetic moments per atom ($\overline{\mu_N}\leqslant 0.7\mu_B$). In contrast, the local moments are expected to be significantly enhanced with respect to the bulk, particularly in the case of Cr, as it is known to be the case at the surfaces of the solid.[19] It is worth noting that if the spins are restricted to be collinear, one generally obtains larger values of $\overline{\mu_N}$, since the sublattice magnetizations often do not cancel out in a finite cluster with an open surface.[3] It would be very interesting to extend the present study by performing realistic d-band model calculations allowing noncollinear spin arrangements in TM clusters, particularly close to half-band filling.

The changes in μ_l and μ_T as a function of U/t are the result of qualitative changes in the magnetic order. As an example we show in Fig. 2 the self-consistent spin arrangements obtained in fcc clusters with $N=13$ atoms for representative values of U/t ($\nu=N$).[20] For small U/t ($U/t<3.7$) one finds a collinear AF order with small μ_l [Fig. 2(a)]. Here we observe a charge- and spin-density wave at the cluster surface that is related to degeneracies in the single-particle spectrum at $U=0$. The atoms belonging to the central (001) plane [shown in gray in Fig. 2(a)] have much larger moments than the atoms at the upper and lower (001) planes. For example, for $U/t=0.5$, $\mu_l=0.13\mu_B$ at the central plane, while the other surface moments are $\mu_l=0.005\mu_B$ (see Fig. 1). The central atom has a small spin polarization ($\mu_1=0.002\mu_B$ for $U/t=0.5$). Notice that the magnetic order within the upper and lower (001) planes is ferromagneticlike (with small μ_l) and that the surface moments belonging to successive (001) planes couple antiferromagnetically. Thus, the magnetic moments at the surface of the central plane are not frustrated since all its NN's are antiparallel to them. This explains qualitatively the larger μ_l found at this plane. In contrast, unavoidable frustrations are found for the smallest magnetic moments at the central site and at the atoms of the upper and lower (001) planes [see Fig. 2(a)].

The crossover from the small-U/t to the large-U/t regime takes place as a succession of noncollinear spin arrangements which attempt to minimize the magnetic frustrations among the increasing local moments. A representative example is shown in Fig. 2(b). While in this case the spin arrangement is noncollinear, all the spin moments still lie in the same plane.

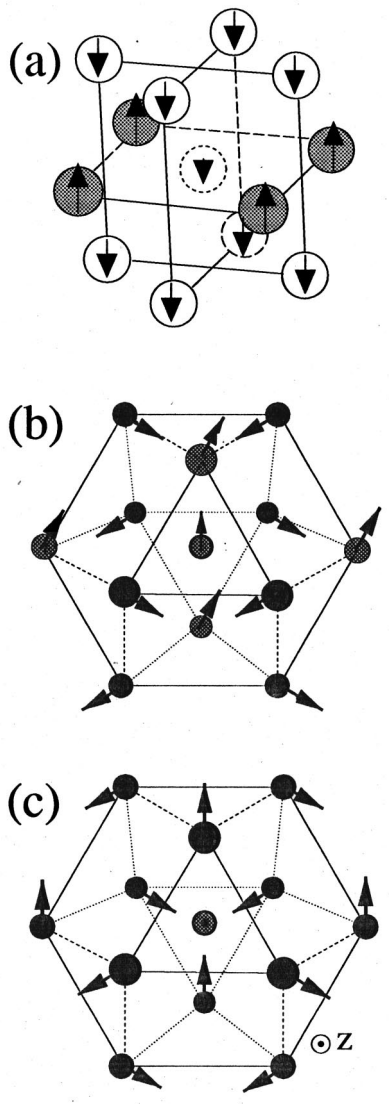

FIG. 2. Illustration of the UHF magnetic order in fcc-like clusters having $N=13$ atoms, $\nu=N=13$ electrons, and representative values of U/t (Hubbard model) (Ref. 20). (a) $U/t<3.7$: the surface atoms in gray have larger local magnetic moments $|\langle\vec{S}_l\rangle|=0.16$–$0.18$ and less electron density $\langle n_l\rangle\simeq 0.88$–$0.90$ than the other surface atoms for which $|\langle\vec{S}_l\rangle|\simeq 0.02$–$0.03$ and $\langle n_l\rangle=1.05$–1.12. The spin arrangement is collinear. (b) $4.8\leqslant U/t<5.1$: the plane of the figure is perpendicular to the (111) direction. The arrows show the local spin polarizations $\langle\vec{S}_l\rangle$ which are all within the (111) plane. (c) $U/t\geqslant 5.1$: the plane of the figure is perpendicular to the (111) direction. The arrows show the projection of $\langle\vec{S}_l\rangle$ on to the (111) plane. At the central atom $\langle\vec{S}_1\rangle\|(111)$. The off-plane components of $\langle\vec{S}_l\rangle$ at the surface atoms are antiparallel to the central spin and have all the same value ($|\langle S_l^z\rangle|\simeq 0.023$–$0.056$ for $l=2$–13).

The very small values of μ_T shown in Fig. 1 for intermediate U/t indicate that there is an almost complete cancellation among the $\langle\vec{S}_l\rangle$. However, this type of spin arrangement is unstable if the strength of Coulomb interactions is further increased. At $U/t\simeq 5.1$ the cluster adopts a fully three-dimensional spin structure which remains essentially unchanged even in the strongly correlated limit [Fig. 2(c)]. The spin arrangement can be viewed as a slight distortion of the spin ordering that minimizes the energy of a classical AF Heisenberg model on the surface shell, i.e., ignoring the interactions with the central site. In fact, if the central atom were removed or if it carried no local moment—as it is the case for $\nu=12$—the surface moments $\langle\vec{S}_l\rangle$ would point along the medians of one of the triangles at the surface and they would lie all within the same plane. The magnetic interactions with the central spin $\langle\vec{S}_1\rangle$ in the 13-atom cluster induce a small tilt $\langle S_l^z\rangle$ of the surface spin polarizations that is opposite to $\langle\vec{S}_1\rangle$ ($\langle\vec{S}_1\rangle\|\hat{z}$ for $\nu=N=13$). The $\langle S_l^z\rangle$ component is the same for all surface sites and depends moderately on U/t ($|\langle S_l^z\rangle|=0.023$–$0.056$ for $U/t\geqslant 5.1$).

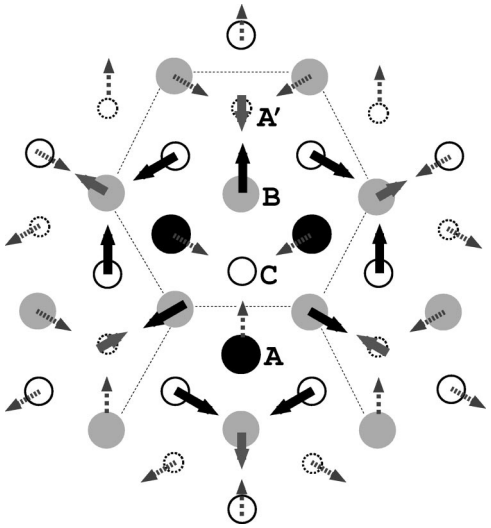

FIG. 3. Illustration of the local magnetic moments $\langle\vec{S}_l\rangle$ in a 43-atom fcc-like cluster at half-band filling and $U/t=10$ (Ref. 20). As in Fig. 2(c), the plane of the figure is perpendicular to the (111) direction. The atoms are represented by circles using different sizes and gray tones for different (111) layers. The latter are denoted by A, B, C, and A′ starting from above. The arrows show the projection of $\langle\vec{S}_l\rangle$ onto the (111) plane. At the central atom $\langle\vec{S}_1\rangle\|(111)$. The spin structure is three-dimensional with off-plane components of $\langle\vec{S}_l\rangle$ that alternate sign on different shells around the central atom. For the 13 innermost atoms the magnetic order is similar to the one shown in Fig. 2(c).

Similar magnetic structures are also found in larger symmetric fcc clusters. In Fig. 3 the self-consistent spin configuration for $N=43$ and $U/t=10$ is illustrated ($\nu=N$). The moment $\langle\vec{S}_1\rangle$ of the central site points along the (111) direction ($\perp$ to the plane of Fig. 3).[20] The other $\langle\vec{S}_m\rangle$ lie almost in the plane of the figure with only small components $\langle S_m^z\rangle$ along the (111) direction. As for $N=13$, $\langle S_m^z\rangle$ is induced by the interactions with $\langle\vec{S}_1\rangle$. In fact, if $\langle\vec{S}_1\rangle$ vanished, all the spins would be in the plane of the figure. $\langle S_m^z\rangle$ is the same for all atoms in a given NN shell, and changes sign as we move from the center to the surface of the cluster. For example, for $U/t=10$, $\cos\theta_{1m}=-0.22$ for m belonging to the first shell, $\cos\theta_{1m}=0.25$ for m in the second shell, and $\cos\theta_{1m}=0.01$ for m in the third shell ($\cos\theta_{lm}=\langle\vec{S}_l\rangle\cdot\langle\vec{S}_m\rangle/|\langle\vec{S}_l\rangle||\langle\vec{S}_m\rangle|$). Notice that the spin ordering of the innermost 13 atoms is very similar to the one found in fcc clusters with $N=13$ [Fig. 2(c)]. While these trends hold for symmetric fcc clusters, it is worth re-

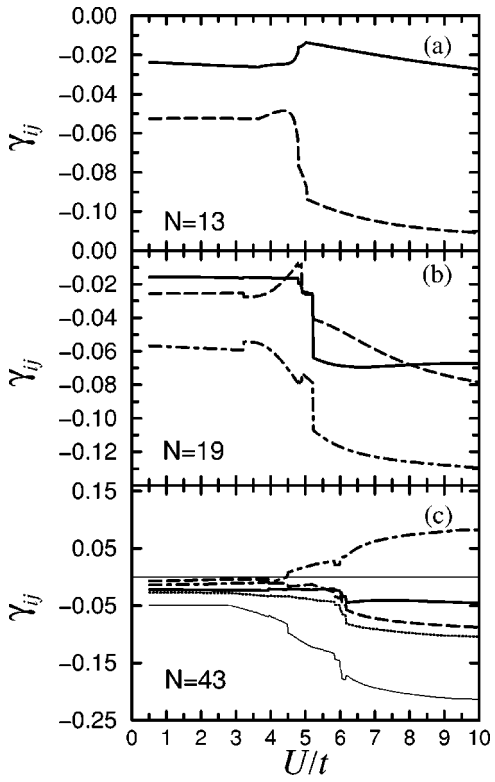

FIG. 4. Spin correlations $\langle \vec{S}_l \cdot \vec{S}_m \rangle$ in fcc-like clusters having $N = 13$–43 atoms as a function of U/t. Results are given for the average spin correlations γ_{01} between the central site and its first NN's (solid), γ_{11} between NN sites on the first shell (dashed), γ_{12} between NN sites on the first and second shell (dashed-dotted), γ_{13} between NN sites on the first and third shell (dotted), and γ_{23} between NN sites on the second and third shell [lower thin curve in (c)].

marking that strong modifications of the magnetic order generally occur if the symmetry of the cluster is lowered. For instance, for $N=14$—an atom added to the closed-shell 13-atom cluster—one obtains a ferromagneticlike coupling between the central atom and some of its first neighbors ($\nu = N$ and $U/t=10$).[21]

A more detailed account of the spin correlations in the UHF ground state of fcc clusters at half-band filling is provided by the expectation values $\langle \vec{S}_l \cdot \vec{S}_m \rangle$. In Fig. 4 the average of $\langle \vec{S}_l \cdot \vec{S}_m \rangle$ between NN atoms at different shells is shown. In most cases we observe that $\langle \vec{S}_l \cdot \vec{S}_m \rangle < 0$ (AF correlations) and that $|\langle \vec{S}_l \cdot \vec{S}_m \rangle|$ increases with increasing U/t. A particularly important increase of AF correlations is observed for intermediate U/t when the local moments μ_l are formed ($U/t \simeq 4.5$–5.5 for $N=13$ and 19, see also Fig. 1). This is consistent with the already discussed decrease of μ_T and the onset of AF order. There are, however, two exceptions to this trend. The correlations γ_{01} between the central site and the surface shell for $N=13$ increase somewhat for $U/t \simeq 5$ ($\gamma_{01}<0$), implying that these AF correlations first tend to be less important when the μ_l increase. This indicates that, as a result of frustrations, the more important increase of AF correlations γ_{11} among the surface NN's is done at the expense of the correlations between the central atom and the surface. A similar behavior is found in exact calculations, as it will be shown in Sec. IV. Another interesting case concerns the correlations γ_{12} between the first and second atomic shells for $N=19$ and 43. Here we observe that γ_{12} changes sign upon going from $N=19$ to $N=43$ ($U/t>5$). Moreover, once the local moments are formed, γ_{01} decreases for $N=19$ [$\gamma_{01}(19)<0$] and increases for $N=43$ as U/t increases [$\gamma_{01}(43)>0$]. This behavior can be qualitatively understood by comparing the surfaces of these clusters. For $N=19$ the outermost spins (shell 2) are free to couple antiferromagnetically with their NN's (shell 1). However, the presence of an additional atomic shell for $N=43$, which has NN's belonging to both the first and second shells, forces a parallel alignment of the spins in shells 1 and 2 in order to allow AF coupling with the third shell. In fact, as shown in Fig. 4(c), γ_{13} and γ_{23} are the strongest AF correlations in the 43-atom cluster. The same conclusions are drawn by comparing the relative orientations of the spin polarizations (Fig. 3). One observes that the angles θ_{23} between NN spin polarizations at shells 2 and 3 are the largest in average ($\theta_{23} \simeq \pi$).

B. Band filling and structural effects

In order to investigate the effect of changing the number of valence electrons close to half-band filling we have performed calculations for fcc-like 13-atom clusters having $\nu = N-1=12$ electrons. One observes that as U/t increases magnetism sets in, showing first a collinear-spin state with small local moments ($U/t \leqslant 4.9$). This corresponds to a spin-density wave along the (001) direction with significant frustrations at triangular faces. As the local moments increase, for larger U/t, the spin arrangement develops an increasing degree of noncollinearity. For $U/t>4.9$ the moments at the triangular faces point along the medians just as in the classical antiferromagnetic ground state of an isolated triangle, yielding a strictly vanishing total moment μ_T.[13] Notice that in spite of the three-dimensional geometry of the cluster, the spin structure is two-dimensional (all magnetic moments lie on the same plane). Qualitatively, these trends are similar to the $\nu=13$ case (Fig. 2). The main difference concerns the behavior at the central site which remains unpolarized as a result of frustrations. As in the $\nu=N$ case (Fig. 1), the small value of the total moment μ_T is the result of noncollinear arrangements of rather large local moments.

The topology and symmetry of the cluster structure are known to play a major role in determining the magnetic correlations within the cluster. It is therefore interesting to consider different geometries and to compare their magnetic behavior. In Fig. 5 the UHF magnetic order in a 13-atom icosahedral cluster having $\nu=12$ electrons is illustrated for representative values of U/t. As a result of degeneracies in the single-particle spectrum ($U=0$) a noncollinear, coplanar arrangement of the local magnetic moments is found at the surface already for very small U/t [see Fig. 5(a) for $0.8 < U/t < 5.5$]. At the central atom (not shown in the figure) the magnetic moment $\mu_1=0$, as in the fcc 13-atom clusters with $\nu=12$. Notice that significant magnetic frustrations are present for small U/t. In some triangles the spin polarizations point along the medians just as in the classical Heisenberg model, while in others two spins are parallel (i.e., fully frustrated) [see Fig. 5(a)]. For larger values of U/t ($U/t > 5.5$) a less frustrated solution is favored by the antiferro-

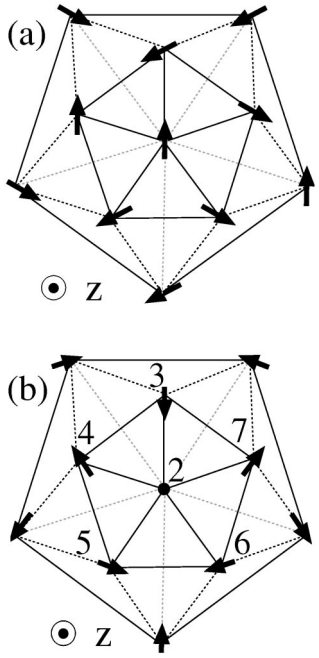

FIG. 5. Illustration of the magnetic order at the surface of an icosahedral 13-atom cluster with $\nu=N-1=12$ electrons (UHF approximation) (Ref. 20). (a) $0.8<U/t\leqslant 5.5$: all local magnetic moments $\langle\vec{S}_l\rangle$, represented by the arrows, are parallel to the plane of the figure. (b) $U/t>5.5$: the arrows show the projections of $\langle\vec{S}_l\rangle$ on the plane of the figure. At site $l=2$, $\langle\vec{S}_l\rangle$ is perpendicular to the plane of the figure (along the z axis). The $\langle\vec{S}_l\rangle$ at sites $l=3-7$ have antiparallel projection to $\langle\vec{S}_2\rangle$ $[\cos\theta_{2l}=(\langle\vec{S}_l\rangle\cdot\langle\vec{S}_2\rangle)/(|\langle\vec{S}_l\rangle||\langle\vec{S}_2\rangle|\simeq-0.45)]$. If brought to a common origin, the spin polarizations $\langle\vec{S}_l\rangle$ form a perfect icosahedron. Notice that the positions of the atoms in the lower pentagonal rings have been expanded along the polar radius in order to ease the visualization.

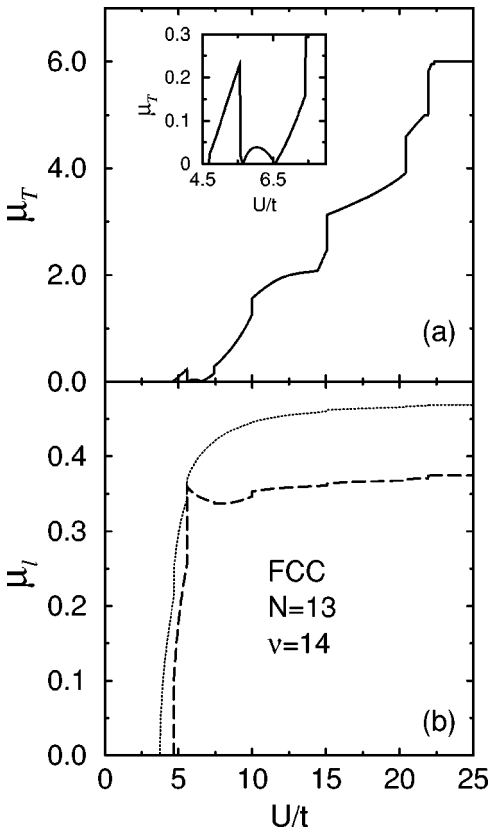

FIG. 6. Magnetic moments in a fcc-like 13-atom cluster with $\nu=14$ electrons as a function of U/t (UHF approximation): (a) total moment $\mu_T=|\Sigma_l\langle\vec{S}_l\rangle|$ and (b) local moments $\mu_l=|\langle\vec{S}_l\rangle|$ at the central site (dashed line) and at the surface (dotted line).

magnetic correlations as shown in Fig. 5(b). This corresponds to a truly three-dimensional arrangement of the surface moments which follows the topology of the cluster geometry ($\mu_1=0$). The spin structure is such that if the surface spin polarizations $\langle\vec{S}_l\rangle$ are brought to a common origin they form an icosahedron. The magnetic moments $\langle\vec{S}_l\rangle$ on pentagonal rings present a small component that is perpendicular to the plane containing the atoms and that is antiparallel to the magnetic moment of the atom capping the ring. The projections of $\langle\vec{S}_l\rangle$ on to the plane of the ring are ordered in the same way as in an isolated pentagon. Once more, very small (in this case strictly vanishing) μ_T is obtained as a result of noncollinear arrangements of rather large local moments $\langle\vec{S}_l\rangle$.

C. Ferromagnetic clusters with noncollinear moments

Strong ferromagnetic systems are described quite correctly in the framework of collinear approaches. In weak (unsaturated) ferromagnets the electronic correlations often result in more complex behaviors. Magnetic instabilities towards noncollinear spin arrangements can be therefore expected in small clusters, particularly in cases of low symmetry or close to a transition from nonmagnetic to ferromagnetic states. In fact, recent first-principles calculations on Fe_N $(N\leqslant 5)$ have revealed new noncollinear spin states than in some cases are more stable than the usually considered collinear ones.[14] In order to investigate this problem we have performed calculations for the band filling $\nu=N+1$ that is known to develop a FM ground state in the limit of large U/t.[22] In Fig. 6 results are given for μ_l and μ_T in an fcc 13-atom cluster with $\nu=14$ electrons. In this case we observe an essentially monotonic increase of μ_T that reflects the progressive development of a fully polarized ferromagnetic state. Close to the threshold for the onset of ferromagnetism $(4.5\leqslant U/t\leqslant 6.5)$ the changes of the AF-like spin arrangement produce small oscillations of μ_T (see the inset of Fig. 6). The approximately steplike behavior resembles at first sight the results obtained in collinear mean-field calculations.[23] However, in the present case the physical picture behind the formation of a FM state is quite different. The increase of μ_T close to the steps involves a succession of noncollinear spin arrangements with increasing degree of parallel moment alignment. Moreover, notice that the local moments increase much more rapidly than μ_T approaching saturation $(\mu_l\simeq 0.40-0.45)$ for values of U/t at which μ_T is still small. Thus, the increase of μ_T with U/t is the result of a progressive parallel alignment of already existing local moments μ_l. In contrast, in collinear Hartree-Fock calculations the increase of μ_T is associated with the formation of the local moments themselves, since μ_T is approximately proportional to μ_l.[23] Comparison with exact calculations shows

that the present noncollinear picture is qualitatively closer to the actual ground-state magnetic properties, at least for the single-band Hubbard model. Indeed, we have computed the local moments $\mu_l^2=\langle S_l^2\rangle$ and the total spin S of the same fcc 13-atom cluster ($\nu=14$) as a function of U/t by using Lanczos exact diagonalization methods.[5,6] Starting from the uncorrelated limit [$\mu_1^2(U=0)=0.28$ and $\mu_l^2(U=0)=0.36$ for $l=2-13$] μ_l^2 increases rapidly with U/t reaching values close to saturation already for $U/t\simeq 10$ [$\mu_1^2(U=10)=0.56$ and $\mu_l^2(U=10)=0.64$ while $\mu_1^2(U=\infty)=0.56$ and $\mu_l^2(U=\infty)=0.70$ for $l=2-13$]. In contrast the ground-state spin S remains equal to zero up to $U/t\simeq 40$. This implies that for $\nu=N+1=14$ the local moments are formed well before FM order sets in, as given by the noncollinear UHF approach (Fig. 6). Notice, however, that the situation could be different for other band fillings where ground-state ferromagnetism is found at much smaller U/t or where S is a nonmonotonous function of U/t [e.g., for $\nu=15-18$ (Ref. 6)]. UHF yields larger local magnetic moments at the cluster surface in agreement with the exact results but it underestimates severely both the Coulomb repulsion U/t above which $\mu_T>1/2$ as well as the U/t for reaching saturation.

The present nonsaturated ferromagnetic behavior with noncollinear spin polarizations is qualitatively analogous to the results recently obtained for small Fe_N clusters ($N\leqslant 5$) in the framework of an unrestricted local spin-density approximation.[14] We have performed calculations using the Hubbard model and UHF for some of the cluster geometries considered in Ref. 14 for Fe_N. In the linear trimer ($N=3$ and $\nu=4$) and in the trigonal bipyramid ($N=5$ and $\nu=6$) the magnetic order changes with increasing U/t from collinear AF, over noncollinear weak FM, to collinear saturated FM, in a similar way as in the previously discussed $N=13$ cluster ($\nu=14$). For intermediate values of U/t we obtain the noncollinear spin arrangements reported in Figs. 1(a) and 1(c) of Ref. 14. The collinear solutions of Ref. 14 are obtained for small U/t [AF as in Fig. 1(b)] or large U/t [FM as in Fig. 1(d)]. This is remarkable, taking into account the significant differences between the first-principles approach and the present one. It suggests that the noncollinear magnetic instabilities should have a more universal origin, probably related to the cluster topology. Finally, it should be recalled that—despite the improvements provided by the fully unrestricted description—the breaking of spin symmetry and the formation of a permanent SDW are artifacts of the mean-field approximation, as demonstrated by exact diagonalization studies for the Hubbard model (see the Sec. IV and Refs. 5 and 6, for example).

IV. COMPARISON BETWEEN UHF AND EXACT RESULTS

A. Spin correlations

In Fig. 7 UHF and exact results are given for the local moments $\mu_l^2=\langle S_l^2\rangle$ and spin correlations $\langle \vec{S}_l\cdot\vec{S}_m\rangle$ in a fcc-like 13-atom cluster. The UHF values for μ_l^2 are quantitatively not far from the exact ones. Not only the uncorrelated limit ($U=0$) is reproduced, but good agreement is also obtained in the large U/t regime. Main trends such as the larger μ_l^2 at the cluster surface for small U/t and the reduction of the difference between surface and inner moments for large U/t are correctly given. However, UHF underestimates the increase of μ_l^2 for $U/t<3.7$ and anticipates the tendency to localization with increasing U/t. This results in a much more rapid crossover from weak to strong interacting regimes than in the exact solution.

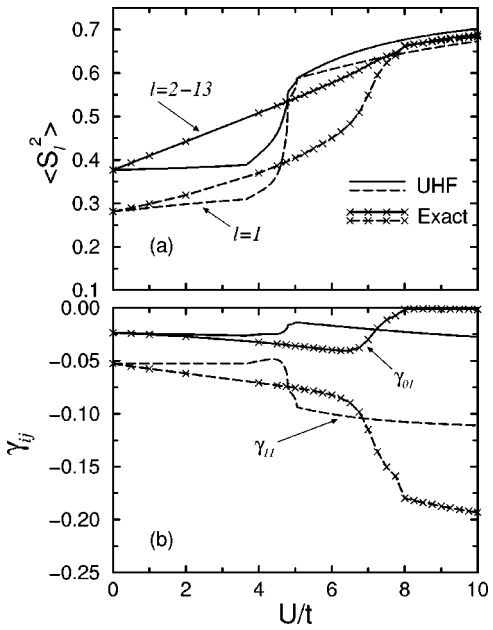

FIG. 7. Comparison between UHF and exact results for a fcc-like 13-atom cluster at half-band filling. (a) Local magnetic moments $\langle S_l^2\rangle$ at the central site ($l=1$, dashed curves) and at the cluster surface ($l=2-13$, solid curves). (b) Average γ_{ij} of the spin correlation functions $\langle \vec{S}_l\cdot\vec{S}_m\rangle$ between the central site and its first NN's at the surface (γ_{01}, solid curves) and between NN's at the surface shell (γ_{11}, dashed curves). The curves with (without) crosses correspond to exact (UHF) results.

The quantitative differences are more important in the case of spin correlation functions $\langle \vec{S}_l\cdot\vec{S}_m\rangle$, particularly for large U/t [Fig. 7(b)]. Here we find that UHF underestimates the strength of AF spin correlations γ_{11} at the surface. This can be interpreted as a consequence of the formation of permanent local moments that blocks quantum spin fluctuations along the transversal directions. Still, in both UHF and exact calculations, the increase of AF correlations at the surface (increase of $|\gamma_{11}|$) is done at the expense of a decrease of the spin correlations with the central atom (decrease of $|\gamma_{01}|$). AF correlations among the larger surface magnetic moments become more dominant, while the AF couplings between the central atom and the different surface atoms tend to cancel out. The discrepancies between UHF and exact results for $N=13$ show the limits of mean-field and give us an approximate idea of the corrections to be expected in correlated calculations on larger clusters. As expected, UHF yields better results for properties like the local moments, that are related to the spin density distribution, than for the correlation functions. Nevertheless, since the trends given by UHF are qualitatively correct, one can be reasonably confident on the validity of the conclusions derived in previous sections for larger clusters (Figs. 1 and 4).

B. Structural stability

The determination of the structure of magnetic clusters is a problem of considerable importance since structure and magnetic behavior are interrelated.[2–6] Moreover, since most calculations of cluster structures are based upon mean-field approximations, it is very interesting to evaluate the role played by the electronic correlations. We have therefore determined the relative stability of a few representative cluster structures as a function of band filling ν/N and Coulomb repulsion strength U/t in the framework of the UHF approximation to the Hubbard model and we have compared the results with available exact calculations.[6] Four different symmetries are considered: icosahedral clusters, which maximize the average coordination number, face-centered-cubic (fcc) and hexagonal-close-packed (hcp) clusters, as examples of compact structures which are found in the solid state, and body-centered-cubic (bcc) clusters, as an example of a rather open bipartite structure. These cluster geometries are representative of the various types of structures found to be the most stable in rigorous geometry optimizations for $N \leqslant 8$.[5]

The results for $N=13$ are summarized in the form of a magnetic and structural diagram shown in Fig. 8. A qualitative description of the type of magnetic order obtained in the self-consistent calculations is indicated by the different shadings. One may distinguish three different *collinear* spin arrangements: nonmagnetic solutions (NM), nonsaturated or weak ferromagnetic solutions (WFM) and saturated ferromagnetic solutions (SFM). The NM case includes paramagnetic states in which the total moment μ_T is minimal ($\mu_T = 0$ or 1/2). Concerning the *noncollinear* spin arrangements we distinguish two cases: noncollinear nonmagnetic states (NC) in which nonvanishing (eventually large) local moments μ_l sum up to an approximately minimal total moment $\mu_T < 1$, and noncollinear ferromagnetic states (NCFM) that show a net magnetization $\mu_T \geqslant 1$. The NC states include all sort of frustrated antiferromagneticlike spin structures, for example, those illustrated in Figs. 2 and 5. In order to quantify the effect of electron correlations the results should be compared with the corresponding magnetic and structural diagram as recently obtained by using exact diagonalization methods (see Fig. 12 of Ref. 6).

For small U/t ($U/t < 10$) the UHF results for the most stable of the considered structures are in very good agreement with the exact calculations (compare Fig. 8 of this paper and Fig. 12 of Ref. 6). The icosahedral cluster yields the lowest energy in the low carrier-concentration regime ($\nu \leqslant 6$) as could have been expected, taking into account that the largest coordination number is favored for small ν.[5] In this case, the kinetic energy dominates (uncorrelated limit) and therefore the structure with the largest bandwidth is stabilized. As ν is increased several structural transitions occur. For small U/t, both exact and UHF calculations present the same structural changes: from icosahedral to fcc structure at $\nu=11$, from fcc to hcp at $\nu=17$, and from hcp to bcc at $\nu=20$. At larger U/t ($U/t > 12$) the interplay between the kinetic and Coulomb energies introduces important correlations that cannot be accounted for within UHF and that play a central role in the determination of the magnetic and structural properties. A main source of discrepancy is the too strong tendency of UHF to yield SFM ground states, particularly above half-band filling, which often disagrees with the exact results.[6] Consequently, the optimal structure is missed rather frequently in the limit of large U/t. For example, for $\nu=19$ and $U/t > 18$, UHF predicts the fcc structure with a SFM ground state, while in the exact calculation the icosahedral cluster with $S=1/2$ is the optimum. Similar drawbacks are seen for other band fillings such as $\nu=7$, 10, 21, and 22 (large U/t). Still, in the event that the true ground state does show strong ferromagnetism, UHF succeeds since the ground state is the superposition of single-particle states. Examples of this kind are $\nu=12$, 14, and 20 for large U/t. These are rather exceptions since the presence of a FM ground state in the exact solution is in general much less frequent than predicted by UHF. Around half-band filling UHF reproduces qualitatively well the transition from fcc or hcp to icosahedral structure with increasing U/t as well as nontrivial reentrant effects ($\nu=13$–18). However, UHF underestimates the value of U/t at which the structural changes occur (see Fig. 8 and Fig. 12 of Ref. 6).

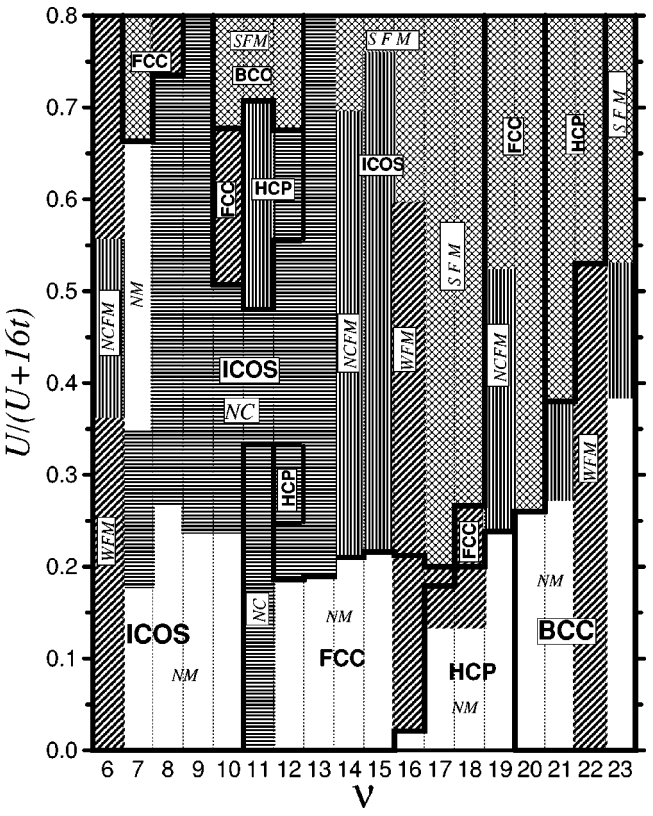

FIG. 8. Magnetic and structural diagram of clusters having $N=13$ atoms as obtained by using the Hubbard model in the unrestricted Hartree-Fock (UHF) approximation. Four different types of structures are considered: icosahedral (ICOS), face-centered-cubic (FCC), hexagonal-close-packed (HCP), and body-centered-cubic (BCC). The lowest-energy structure is given as a function of the Coulomb repulsion strength U, hopping integral t, and number of electrons ν. The bold lines indicate the structural transitions. For $\nu<6$ the lowest-energy structure is icosahedral and for $\nu>23$ it is bcc. The corresponding UHF magnetic orders are indicated by different shading patterns: nonmagnetic (no shading, NM), collinear weak ferromagnetic (diagonal lines, WFM), saturated ferromagnetic (crossed lines, SFM), noncollinear with total moment $\mu_T<1$ (horizontal lines, NC), and noncollinear with total moment $\mu_T \geqslant 1$ (vertical lines, NCFM).

V. SUMMARY AND OUTLOOK

The magnetic properties of compact clusters have been investigated using the single-band Hubbard model and the fully unrestricted HF approximation that allows the formation of noncollinear arrangements of the local magnetic moments $\langle \vec{S}_l \rangle$. AF clusters in the relevant interaction regime ($U/t > 5$) show large $\langle \vec{S}_l \rangle$ forming complex spin arrangements that attempt to minimize the effects of frustrations in the compact (nonbipartite) structure. The resulting cluster magnetization $\mu_T = |\Sigma_l \langle \vec{S}_l \rangle|$ is in general very small or vanishing. This is a significant improvement with respect to collinear studies and agrees qualitatively with exact results. The details of the magnetic order are found to be very sensitive to the topology of the cluster geometry.

A new physical picture has been obtained for the development of ferromagnetism in small clusters with increasing U/t. In contrast to previous collinear calculations—where the local moments and ferromagnetism develop simultaneously[23]—the FM state is built up by the progressive alignment of already existing local moments $\mu_l = |\langle \vec{S}_l \rangle|$. The validity of this interpretation is supported by exact results for $N = 13$ and $\nu = 14$ which shows that local moments are present at values of U/t far smaller than those required for the formation of a FM ground-state ($S \geqslant 1$). A similar behavior is expected for more realistic multiband models and for other low-dimensional systems.

Concerning the structural stability, we have shown that UHF fails to reproduce the exact phase diagram in detail, particularly in some of the most interesting AF or weak FM regimes. Structural transitions are sometimes missing and in other cases changes of structures appear artificially. Nevertheless, it is also fair to say that UHF yields a good account of the relative stability between the considered structures, even well beyond the weakly interacting regime (up to $U/t \simeq 16$), and that it also explains the larger stability of ferromagnetism above half-band filling. In the limit of very strong interactions the validity of UHF breaks down and correlation effects beyond the single-determinant wave function are indispensable in order to obtain the ground-state structure and magnetic behavior reliably.

The role of electron correlations on the magnetic behavior has been quantified by comparison with exact diagonalizations for $N = 13$ atoms. Despite some quantitative discrepancies, the U/t and environment dependences of the local magnetic moments and spin correlation functions given by UHF are in good qualitative agreement with the exact results. This suggests that UHF with noncollinear spin arrangements is a valid starting point for working on larger clusters and more complex multiband models. It would be very interesting to extend the present approach to realistic *d*-band models in order to allow a direct comparison with experiments and first principles calculations on TM clusters. Noncollinear effects are expected to be particularly important for TM's showing a tendency to antiferromagnetism such as Cr_N,[25] V_N, Mn_N,[26] or $(Fe_xCr_{1-x})_N$,[24] as well as for weak FM systems such as Rh_N.[2] Deviations from collinearity should also play a role as finite-temperature spin excitations in the more conventional FM materials (Fe_N, Co_N, and Ni_N).

Improvements on the UHF wave function could be introduced by restoring the broken spin symmetry as proposed in Refs. 17 and 18. However, the success of such an approach is likely to depend on the geometry of the cluster. For example, in low symmetry structures UHF tends to exaggerate the formation of spin- and charge-density redistributions. This may be far from the actual exact solution and can be difficult to correct *a posteriori*. In such cases a Jastrow-like variational ansatz on restricted Hartree-Fock states would seem more appropriate. Finally, it should be recalled that the Hubbard model for small clusters with one orbital per site is probably the most extremely low-dimensional system one may consider. Therefore, fluctuations and correlations effects are expected to be here more drastic than in larger clusters or in realistic multiband models, more appropriate for the description of TM's.

ACKNOWLEDGMENTS

This work has been financed in part by CONACyT (Mexico) and CNRS (France). M.A.O. acknowledges support from CONACyT (Mexico) and FAI (UASLP). G.M.P. acknowledges support from the J. S. Guggenheim Memorial Foundation.

[1] See, for instance, *Proceedings of the 8th International Symposium on Small Particles and Inorganic Clusters (ISSPIC), Copenagen, Denmark, 1996*, edited by H.H. Andersen (Springer, New York, 1997), Vol. XVI; Proceedings of the 9th International Symposium on Small Particles and Inorganic Clusters (ISSPIC-9), Lausanne, Switzerland, 1998 [Eur. Phys. J. D (to be published)].

[2] D.R. Salahub and R.P. Messmer, Surf. Sci. **106**, 415 (1981); C.Y. Yang, K.H. Johnson, D.R. Salahub, J. Kaspar, and R.P. Messmer, Phys. Rev. B **24**, 5673 (1981); K. Lee, J. Callaway, and S. Dhar, *ibid.* **30**, 1724 (1985); K. Lee, J. Callaway, K. Wong, R. Tang, and A. Ziegler, *ibid.* **31**, 1796 (1985); B.I. Dunlap, Z. Phys. D **19**, 255 (1991); J.L. Chen, C.S. Wang, K.A. Jackson, and M.R. Perderson, Phys. Rev. B **44**, 6558 (1991); M. Castro and D.R. Salahub, *ibid.* **49**, 11 842 (1994); P. Ballone and R.O. Jones, Chem. Phys. Lett. **233**, 632 (1995); B.V. Reddy, S.N. Khanna, and B.I. Dunlap, Phys. Rev. Lett. **70**, 3323 (1993); B. Piveteau, M-C. Desjonquéres, A.M. Olés, and D. Spanjaard, Phys. Rev. B **53**, 9251 (1996); J. Dorantes-Dávila, P. Villaseñor-González, H. Dreyssé, and G.M. Pastor, *ibid.* **55**, 15 084 (1997).

[3] G.M. Pastor, J. Dorantes-Dávila, and K.H. Bennemann, Physica B **149**, 22 (1988); Phys. Rev. B **40**, 7642 (1989); J. Dorantes-Dávila and H. Dreyssé, *ibid.* **47**, 3857 (1993); K. Lee and J. Callaway, *ibid.* **48**, 15 358 (1993); P. Alvarado, J. Dorantes-Dávila, and H. Dreyssé, *ibid.* **50**, 1039 (1994); Hansong Cheng and Lai-Sheng Wang, Phys. Rev. Lett. **77**, 51 (1996).

[4] L.M. Falicov and R.H. Victora, Phys. Rev. B **30**, 1695 (1984); Y. Ishii and S. Sugano, J. Phys. Soc. Jpn. **53**, 3895 (1984); J. Callaway, D.P. Chen, and R. Tang, Z. Phys. D **3**, 91 (1986); Phys. Rev. B **35**, 3705 (1987).

[5] G.M. Pastor, R. Hirsch, and B. Mühlschlegel, Phys. Rev. Lett. **72**, 3879 (1994); Phys. Rev. B **53**, 10 382 (1996).

[6] F. López-Urías and G.M. Pastor, Phys. Rev. B **59**, 5223 (1999).
[7] D.R. Penn, Phys. Rev. **142**, 350 (1966).
[8] F. Keffer, in *Encyclopedia of Physics*, edited by H.P.J. Wijn (Springer, Berlin, 1966), Vol. 18, p. 2; Y. Tsunoda, J. Phys.: Condens. Matter **1**, 10 427 (1989).
[9] M.V. You and V. Heine, J. Phys. F **12**, 177 (1982).
[10] R. Lorenz, J. Hafner, S.S. Jaswal, and D.J. Sellmyer, Phys. Rev. Lett. **74**, 3688 (1995); A.V. Smirnov and A.M. Bratkovsky, Europhys. Lett. **33**, 527 (1996); L.M. Sandratskii and J. Kübler, Phys. Rev. Lett. **76**, 4963 (1996); L. Nordström and D.J. Singh, *ibid.* **76**, 4420 (1996).
[11] J.A. Vergés, E. Louis, P.S. Lommdahl, F. Guinea, and A.R. Bishop, Phys. Rev. B **43**, 6099 (1991); E. Louis, F. Guinea, and J.A. Vergés, Phys. Scr. **T39**, 140 (1991), and references therein; J.A. Vergés, F. Guinea, and E. Louis, Phys. Rev. B **46**, 3562 (1992).
[12] D. Coffey and S.A. Trugman, Phys. Rev. Lett. **69**, 176 (1992); F. Willaime and L.M. Falicov, J. Chem. Phys. **98**, 6369 (1993); L. Bergomi, J.P. Blaizot, Th. Jolicoeur, and E. Dagotto, Phys. Rev. B **47**, 5539 (1993).
[13] M.A. Ojeda-López, J. Dorantes-Dávila, and G.M. Pastor, J. Appl. Phys. **81**, 4170 (1997).
[14] T. Oda, A. Pasquarello, and R. Car, Phys. Rev. Lett. **80**, 3622 (1998).
[15] D.C. Douglass, J.P. Bucher, and L.A. Bloomfield, Phys. Rev. B **45**, 6341 (1992).
[16] J. Hubbard, Proc. R. Soc. London, Ser. A **276**, 238 (1963); **281**, 401 (1964); J. Kanamori, Prog. Theor. Phys. **30**, 275 (1963); M.C. Gutzwiller, Phys. Rev. Lett. **10**, 159 (1963).
[17] L.M. Falicov and R.A. Harris, J. Chem. Phys. **51**, 3153 (1969).
[18] S.L. Reindl and G.M. Pastor, Phys. Rev. B **47**, 4680 (1993).
[19] G. Allan, Surf. Sci. **74**, 79 (1978); H. Hasegawa, J. Phys. F **16**, 1555 (1986); L.E. Klebanoff, S.E. Robey, G. Liu, and D.A. Shirley, Phys. Rev. B **30**, 1048 (1984); L.E. Klebanoff, R.H. Victora, L.M. Falicov, and D.A. Shirley, *ibid.* **32**, 1997 (1985); A.A. Aligia, J. Dorantes-Dávila, J.L. Morán López, and K.H. Bennemann, *ibid.* **35**, 7053 (1987).
[20] In the present model without spin-orbit interactions the energy is invariant after any rotation of the complete spin arrangement with respect to the cluster structure. Only the relative orientations of the $\langle \vec{S}_l \rangle$ are significant. The choice made in the figures is arbitrary and obeys only illustrative purposes.
[21] M.A. Ojeda-López, Ph.D. thesis, Universidad Autónoma de San Luis Potosí, Mexico, 1998.
[22] Y. Nagaoka, Solid State Commun. **3**, 409 (1965); D.J. Thouless, Proc. Phys. Soc. London **86**, 893 (1965); Y. Nagaoka, Phys. Rev. **147**, 392 (1966); H. Tasaki, Phys. Rev. B **40**, 9192 (1989).
[23] J. Dorantes-Dávila, H. Dreyssé, and G.M. Pastor, Phys. Rev. B **46**, 10 432 (1992).
[24] A. Vega, J. Dorantes-Dávila, G.M. Pastor, and L.C. Balbás, Z. Phys. D **19**, 263 (1991).
[25] C. Kohl and G.F. Bertsch (unpublished).
[26] M.R. Pederson, F. Reuse, and S.N. Khanna, Phys. Rev. B **58**, 5632 (1998).